Article

Characteristic Metabolites and Antioxidant Activities of Essential Oils from Phlomoides rotata (Benth. ex Hook. f.) Mathiesen

Zheng Pan , Chen Xie , Jie Luo , Xiao Tong Yan , Yong Mei Su , Anwar Ul Haq , Nasir Mehmood Khan , Shujaat Ahmad , Jian Wang *

Posted Date: 9 February 2024

doi: 10.20944/preprints202402.0584.v1

Keywords: Phlomoides rotata (Benth. ex Hook. f.) Mathiesen (Lamiophlomis rotata (Benth.) Kudô); essential oils; characteristic metabolites; metabolomics; fatty acids; C13-norisoprenoids; biosynthesis; antioxidant activities; pro-oxidant activities

Article

Characteristic Metabolites and Antioxidant Activities of Essential Oils from *Phlomoides rotata* (Benth. ex Hook. f.) Mathiesen

Zheng Pan [1,2], Chen Xie [1,2], Jie Luo [1,2], Xiaotong Yan [1,2], Yongmei Su [1,2], Anwar Ul Haq [3], Nasir Mehmood Khan [4], Shujaat Ahmad [3] and Jian Wang [1,2,5,*]

[1] College of Chinese Medicine, Chongqing Medical University, Chongqing 400016, China; 102796@cqmu.edu.cn (Z.P.); 2022110750@stu.cqmu.edu.cn (C.X.); 2023121966@stu.cqmu.edu.cn (J.L.); yxt2438249780@163.com (X.Y.); 101817@cqmu.edu.cn (Y.S.)

[2] Chongqing Key Laboratory of Chinese Medicine for Prevention and Cure of Metabolic Diseases, Chongqing Medical University, Chongqing 400016, China

[3] Department of Pharmacy, Shaheed Benazir Bhutto University, Sheringal, Upper Dir 18000, Khyber Pakhtunkhwa, Pakistan; anwar@sbbu.edu.pk (A.U.H.); shujaat@sbbu.edu.pk (S.A.)

[4] Department of Agriculture, Shaheed Benazir Bhutto University, Sheringal, Upper Dir 18000, Khyber Pakhtunkhwa, Pakistan; nasir@sbbu.edu.pk

[5] Department of Chinese Materia Medica, Chongqing College of Traditional Chinese Medicine, Chongqing 402760, China

* Correspondence: wj_2000_abc@cqmu.edu.cn

Abstract: Limited research has been conducted on the metabolites present in the essential oils (Es) of *Phlomoides rotata* (Benth. ex Hook. f.) Mathiesen (PR, syn. *Lamiophlomis rotata* (Benth.) Kudô), and their potential pharmacological activities, such as antioxidant and anticancer properties, are often overlooked. We conducted a metabolomics-based screening to identify the characteristic metabolites (CMs) present in the Es extracted from PR. Furthermore, we evaluated their *in vitro* antioxidant activities (AOAs). The Es obtained through hydro-distillation are characterized by a light yellow color and a fresh, elegant fragrance. Cryoprecipitation was used to separate the crystals (Cs) from the Es, resulting in the extraction of crystal-free essential oils (CFs). A total of 107 components belonging to 8 categories were identified and quantified in the Es, Cs, and CFs using GC-MS and GC-FID techniques. Among these components, 76 were reported for the first time in the Es of PR. The major compounds identified include long-chain fatty acids (LCFAs) and their esters, such as palmitic acid (PA), myristic acid (MA), linoleic acid (LA), oleic acid (OA), and methyl palmitate. Additionally, seven C13-norisoprenoids, with *trans*-*β*-damascenone being particularly notable for its flavor, were also identified. A sum of nine CMs were identified in the Es, including PA, MA, LA, OA, methyl palmitate, hexahydrofarnesyl acetone, phytol, *trans*-*β*-damascenone, and hexanal. The main metabolic pathway in the Es is the biosynthesis of FAs and terpenoids revealed by MetaboAnalyst 6.0 and KEGG analyses. Furthermore, the *in vitro* AOAs of the Es, Cs, CFs, and four selected CMs (PA, MA, LA, and OA) were evaluated. Generally, PA and MA exhibited pro-oxidant activities (POAs) or weak AOAs. LA and OA demonstrated POAs or weak AOAs at lower concentrations, but at higher concentrations, they displayed medium to strong AOAs. Importantly, the CFs exhibited stronger AOAs compared to the corresponding Es, which may be attributed to their different PA content. Overall, this study provides valuable insights into the potential utilization of Es from PR.

Keywords: *Phlomoides rotata* (Benth. ex Hook. f.) Mathiesen (*Lamiophlomis rotata* (Benth.) Kudô); essential oils; characteristic metabolites; metabolomics; fatty acids; C13-norisoprenoids; biosynthesis; antioxidant activities; pro-oxidant activities

 doi:10.20944/preprints202402.0584.v1

1. Introduction

Phlomoides rotata (Benth. ex Hook. f.) Mathiesen (PR), also known as *Lamiophlomis rotata* (Benth.) Kudô, is a medicinal herb called "Duyiwei" (*Lamiophlomis herba*) in Chinese. It belongs to the *Phlomoides* Moench of Lamiaceae and is found in high altitudes in China [1–4]. Traditionally, the root, rhizome, or the entire herb were used for medicinal purposes [5,6]. However, nowadays, only the aerial parts are used [4], and the digging of the root is prohibited due to PR being listed as a first-class endangered Tibetan medicine [6,7]. The underground parts of PR are known for promoting blood circulation, eliminating stasis, reducing swelling, and providing analgesic effects. The above-ground parts are used for treating grasserie, fractures, injuries from falls, osteomyelitis, gunshot injuries, and edema pain [2,5–7]. *Lamiophlomis herba* is yellowish-brown or sallow, with a bitter and flat taste [4,5,7]. It was first documented in the classical masterpiece of Tibetan Medicine, Somaratsa [7], and has been used for more than 2000 years in traditional Tibetan medicine, known as "Daba" and "Dabuba," to treat traumatic injuries, rheumatic arthritis (RA), and grasserie [4–7]. In clinical practice, PR is typically used directly without any prior processing, mainly for pain relief [6]. Additionally, PR is commonly used as a key ingredient in combination with other Chinese herbs such as *Curcuma longa*, *Salvia miltiorrhiza*, and *Pyrrosia lingua* [6,7]. PR is also utilized as an ingredient in various health products, including health drinks, soap, wine, mouth rinses, and biological toothpastes [6].

Due to the low content of volatile chemicals, the focus of research on PR has primarily been on its involatile compounds. So far, at least 223 chemical constituents have been isolated from PR, including iridoids, flavonoids, phenylethanoid glycosides, polysaccharides, organic acids, volatile oils, and others [6,7]. The main compounds found are iridoid glycosides, which are responsible for the analgesic effect [6,7] and serve as characteristic metabolites (CMs) to assess the quality of Duyiwei [7]. However, C13-norisoprenoids have been largely overlooked, with only one previously reported compound, 5β, 6α-dihydroxy-3β-(β-D-glucopyranosyloxy)-7-megastigmen-9-one [8]. Additionally, fourteen organic acids, including palmitic acid (PA), have been isolated and identified [6]. As of now, there is only one published study that has reported the chemical composition of the essential oils (Es) extracted from PR using steam distillation, and another study has reported the lipophilic composition in the CH_2Cl_2 extracted part. Additional details and data can be found in supplemental Table S1 [9,10]. The main compounds found in terms of content are fatty acids (FAs), especially long-chain FAs such as PA, myristic acid (MA), oleic acid (OA), and linoleic acid (LA). However, some identifications are still debatable, such as OA, linoleic acid ethyl ester, and cyclohexenylacetic acid, taking into consideration the values of linear retention indices (LRIs) and the mass spectra [9,10]. Only three compounds, MA, PA, and LA, were detected in both studies [9,10]. The identification of CMs from PR EOs is of great importance as these CMs play a crucial role in distinguishing these EOs from others rapidly [11–13].

In recent years, there have been limited studies on the in-depth biological effects of volatile oils from PR [7]. However, the petroleum ether extracted part has been reported to possess anti-tumor activities, suggesting that the volatile compounds may also have such activities [14]. Currently, there have been no tests conducted on the antioxidant activities (AOAs) of volatile chemicals extracted from PR. Oxidative stress has been associated with various diseases, including RA, cancer, and diabetes [15,16]. Additionally, supplemental FAs play an important role in maintaining the balance between oxidation and antioxidation in cells [17–24]. The effects of FAs on oxidant injury seem to be linked to the degree of unsaturation [18]. PA, a type of saturated FAs (SFAs), can increase oxidative stress in cells in a concentration-dependent manner [23,24]. This is because it can induce overexpression of the pro-oxidant protein p66Shc [23] or react with cells to generate reactive oxygen species (ROS), reduce the content of NO, and make cells more susceptible to oxidative stress [24]. On the other hand, stearic acid, another type of SFAs, has been reported to protect pulmonary artery endothelial cells from oxidant injury [18]. Generally, polyunsaturated FAs (PUFAs) can reduce oxidant injury [19–22], although contradictory results have also been reported [18].

To the best of our knowledge, no single extract or compound from PR has been clinically applied for disease treatment thus far. Therefore, it is necessary to conduct studies and develop potentially

 doi:10.20944/preprints202402.0584.v1

therapeutic extracts or compounds [7]. Building upon previous research [25], our focus in this study is on the volatile chemicals and their AOAs. We have selected three samples of PR from Tibet to evaluate the CMs present in the Es and their AOAs. The process involved isolating crystals (Cs) from the Es using cryoprecipitation, which resulted in crystal-free Es (CFs). Subsequently, a comprehensive chemical profiling study was conducted on the Es, Cs, and CFs using GC-MS and GC-FID techniques. Additionally, *in vitro* assays have been conducted to assess the AOAs of the Es, separated parts, and four CMs, namely PA, MA, LA, and OA. The findings of this study will contribute to establishing a theoretical foundation for the utilization of PR Es.

2. Results

2.1. Extraction and separation

From PR with Voucher No. L8, L9, and L10, a total of 0.29 g, 0.26 g, and 0.19 g of light yellow Es were obtained, corresponding to 418 μL, 405 μL, and 238 μL, respectively. The yields of the Es were calculated as 0.13%, 0.13%, and 0.08%, respectively, based on the ratio of the volume of the Es (in mL) to the weight of the PR (in g) (mL/g). The densities of the Es were measured as 0.69, 0.64, and 0.8, respectively. These Es have a fresh and elegant smell. Crystals were separated from the EOs at temperatures of 4 °C or -4 °C. The EOs were then obtained by removing the crystals.

2.2. Chemical composition of the Es from PR

A total of 107 compounds have been qualified and quantified, as indicated in supplemental Table S2 and Figure 1.

 doi:10.20944/preprints202402.0584.v1

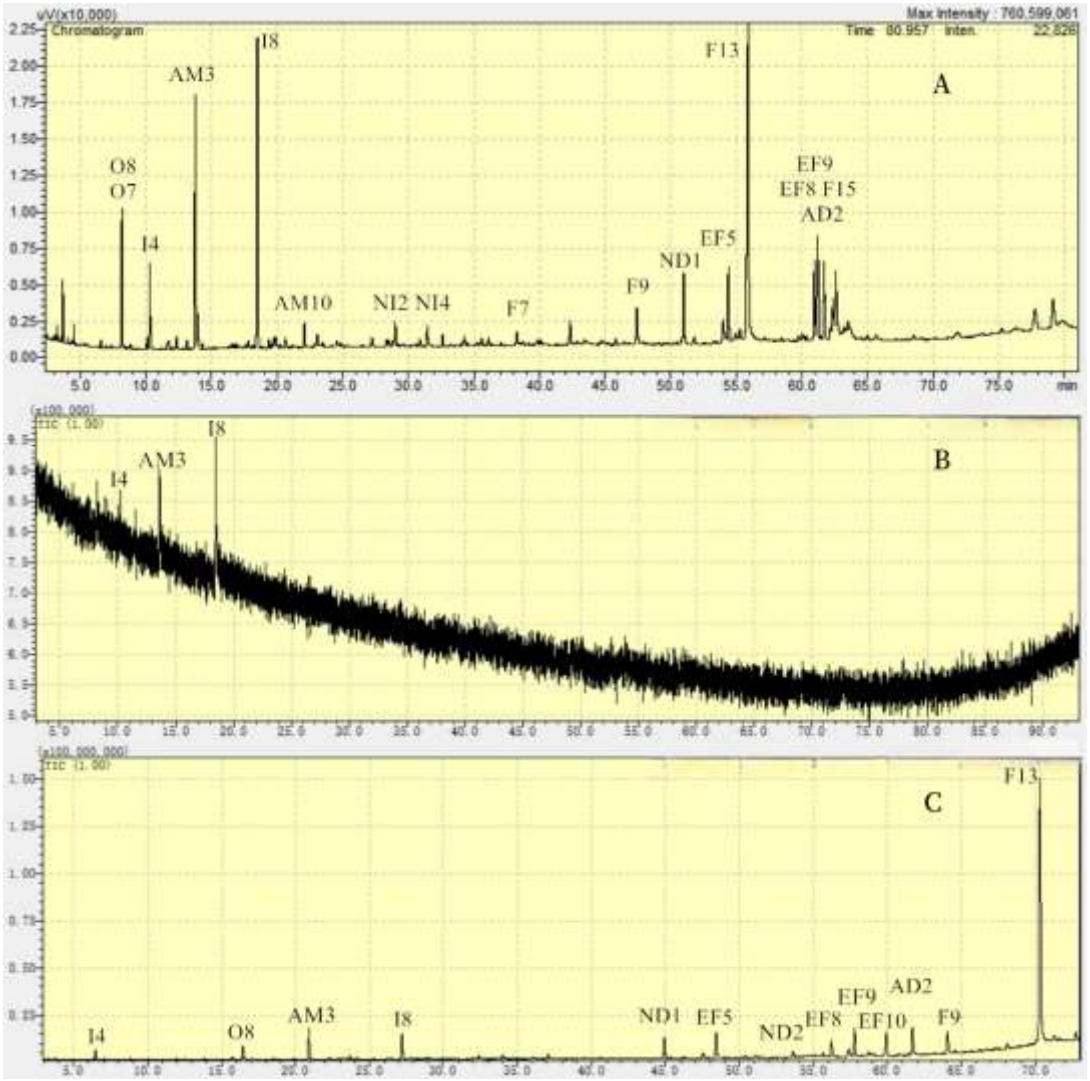

Figure 1. The chromatograms of E10. A, B, and C were detected using a DB-5 column in gas chromatography with flame ionization detector (GC-FID) and gas chromatography-mass spectrometer (GC-MS) setups, as well as a free FA phase (FFAP) column in a GC-MS system, respectively. Each denoted compound is assigned the corresponding code as listed in Supplementary Table S2.

A total of 107 compounds have been both qualified and quantified. Among them, 31 compounds have been previously reported [9,10], while 76 compounds are being reported for the first time from the EOs of PR. These compounds belong to various classes, including FAs, esters of FAs, C13-norisoprenoids, AMs, C18-norditerpenoids, ADs, Als, Others, and Introduced. The relative contents of these compounds are listed in Figure 2.

 doi:10.20944/preprints202402.0584.v1

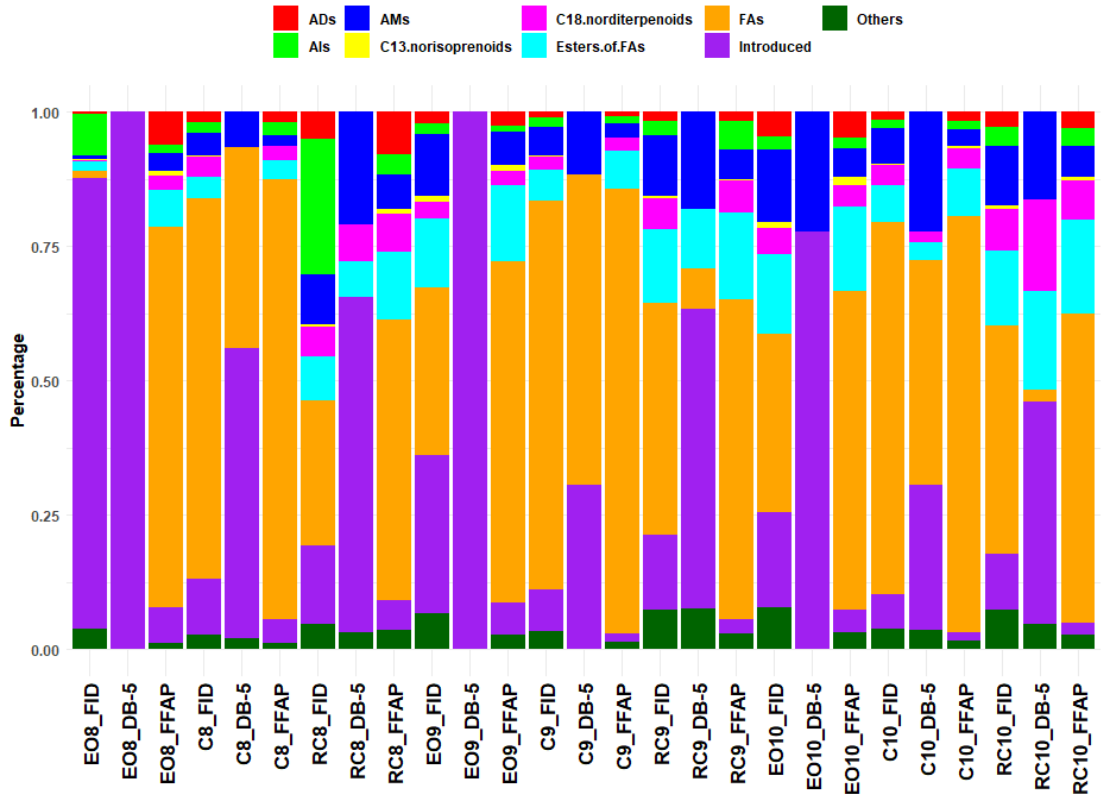

Figure 2. The content of each class compound.

Due to the low concentrations of samples, only eight compounds were detected by GC-MS using DB-5. These compounds include hexanal, 1-octen-3-ol, limonene, linalool, α-terpineol, hexahydrofarnesyl acetone, methyl palmitate, and PA. Among them, the contents of limonene, α-terpineol, and PA are relatively high.

The 9-hexadecenoic acid reported previously [9] is most likely corresponding to the 9*E*-hexadecenoic acid detected in this study, based on their LRIs values.

The EOs, crystals, and EOs free of crystals primarily consist of FAs, particularly LCFAs. PA stands out as the most prominent FA, which aligns with the reported findings [9,10]. Additionally, MA, OA, and LA are also significant, as previously reported [9,10]. The content of PA is relatively higher in crystals but relatively lower in EOs free of crystals compared to the corresponding EOs.

Regarding the esters of FAs, the major compounds are methyl palmitate, methyl oleate, methyl linoleate, and methyl linolenate.

These seven types of C13-norisoprenoids are being reported for the first time from the EOs of PR. Their content is relatively low, and the content in the EOs is relatively higher compared to that in the corresponding crystals or EOs free of crystals.

Among the AMs, linalool is relatively prominent. Within the C18-norditerpenoid group, hexahydrofarnesyl acetone stands out. Phytol is a noteworthy ADs. Tricosane and pentacosane are two notable Als. In addition, compounds such as hexanal, 1-octen-3-ol, and β-caryophyllene should also be observed. A total of eight compounds, including limonene, α-terpineol, β-pinene, β-myrcene, *p*-cymene, γ-terpinene, isoterpinolene, and terpinen-4-ol, are likely introduced from the EOs extracted from the peels of Nanfengmiju (*Citrus kinokuni* Hort. ex Tanaka), a variety of *C. reticulata*, which were studied simultaneously [11].

 doi:10.20944/preprints202402.0584.v1

2.3. Principal Component Analysis (PCA) and Partial Least Squares Discriminant Analysis (PLS-DA) of the metabolites in Es of PR

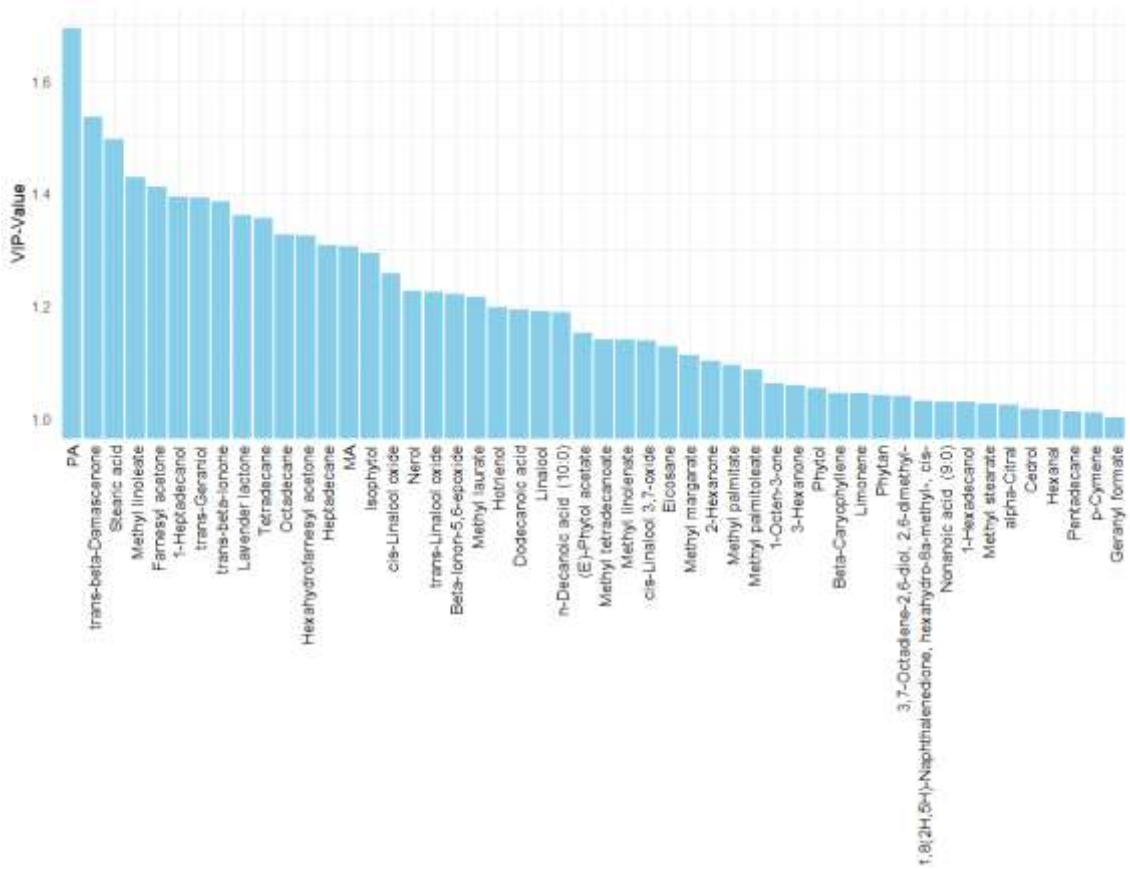

Figure 3. A total of 50 compounds were screened based on the data obtained by GC-FID and GC-MS with a FFAP column. The screening standard required a VIP (Variable Importance in Projection) value of not less than 1.

 doi:10.20944/preprints202402.0584.v1

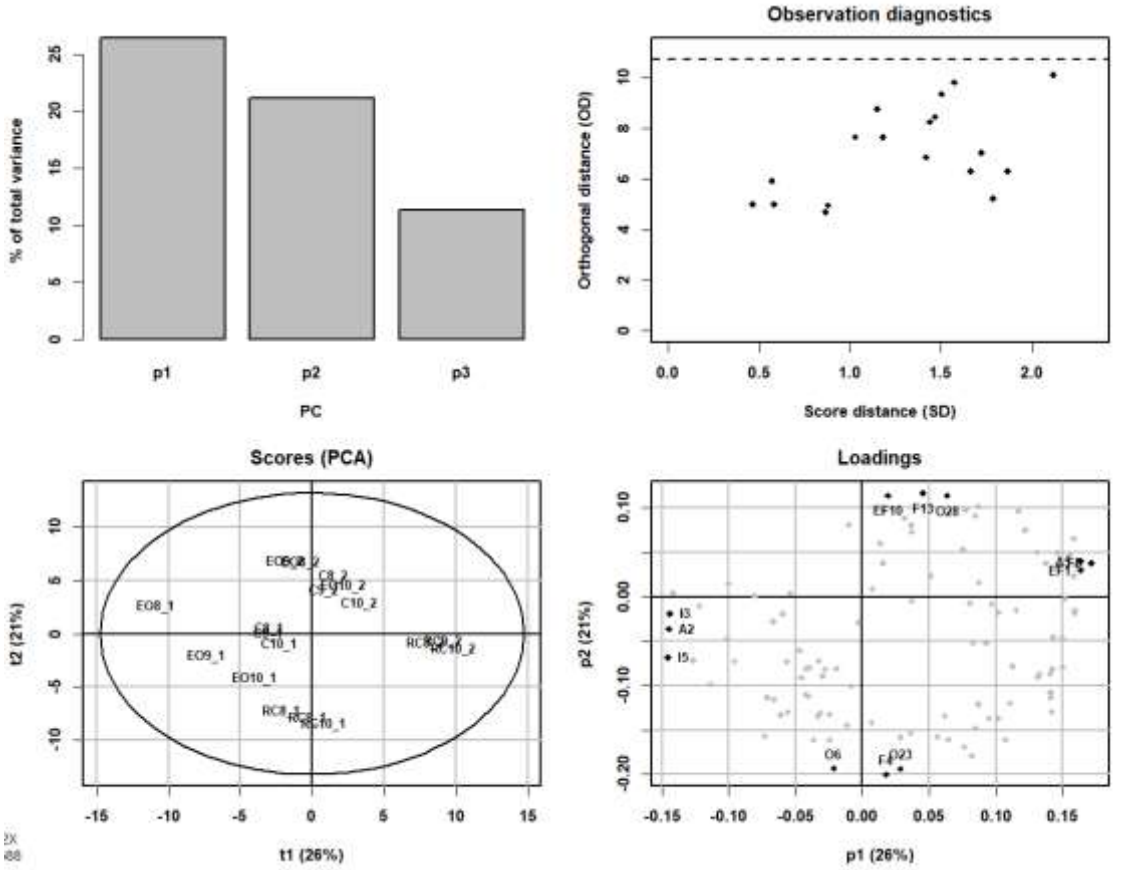

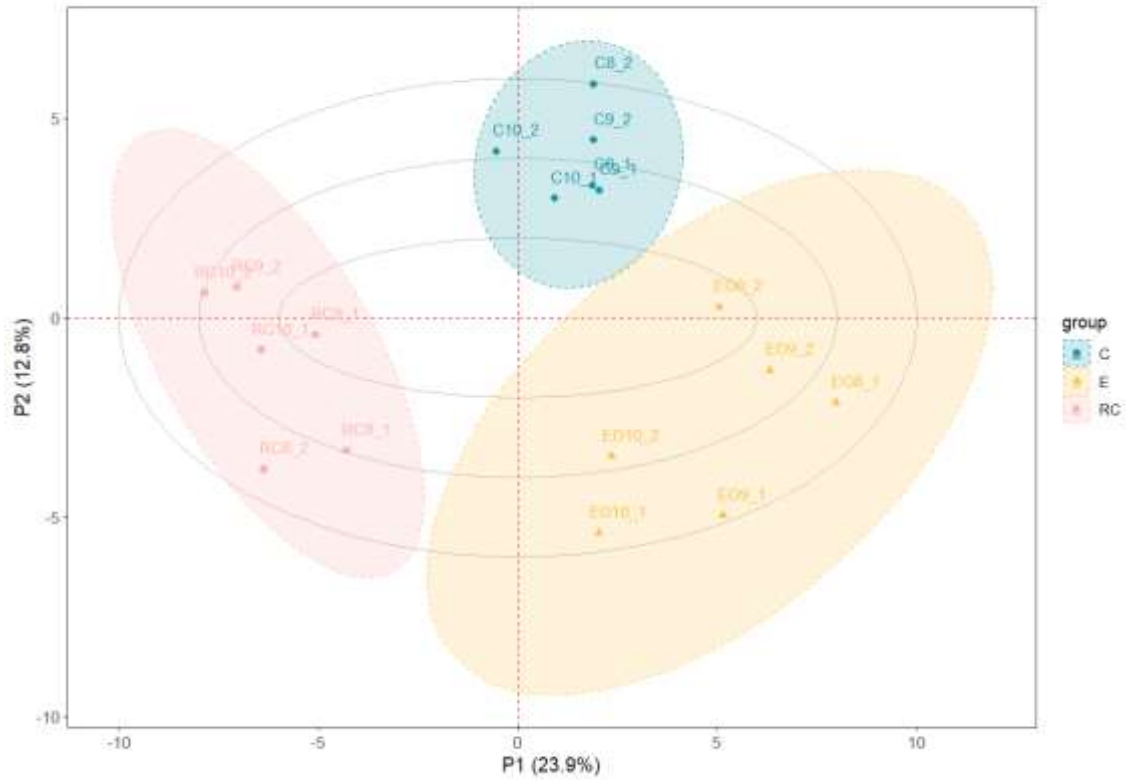

 doi:10.20944/preprints202402.0584.v1

Figure 4. PCA and PLS-DA plots. In the sample names, the "_1" and "_2" indicate that the data was obtained from GC-FID and GC-MS with a FFAP column, respectively. The compounds represented in the loadings of the PCA plot are as follows: EF10 - Methyl linolenate, F13 - PA, O28 - 1,8(2H,5H)-Naphthalenedione, hexahydro-8a-methyl-, *cis*-, EF1 - Nonanoic acid, 9-oxo-, methyl ester, A5 - Hexadecane, F8 - Tridecanoic acid, O6 - Hexanal, F4 - Nonanoic acid, O23 - Cedrol, I3 - *p*-Cymene, A2 - Farnesane, I5 - γ-Terpinene.

It is evident that within each group, the six samples are relatively closer to each other, while between the groups, they are relatively less close.

2.4. Metabolic pathway analysis

As shown in Figure 5, the metabolite pathway listed in sequence are fatty acid biosynthesis, biosynthesis of unsaturated fatty acids, cutin, suberine and was biosynthesis, fatty acid elongation, fatty acid degradation.

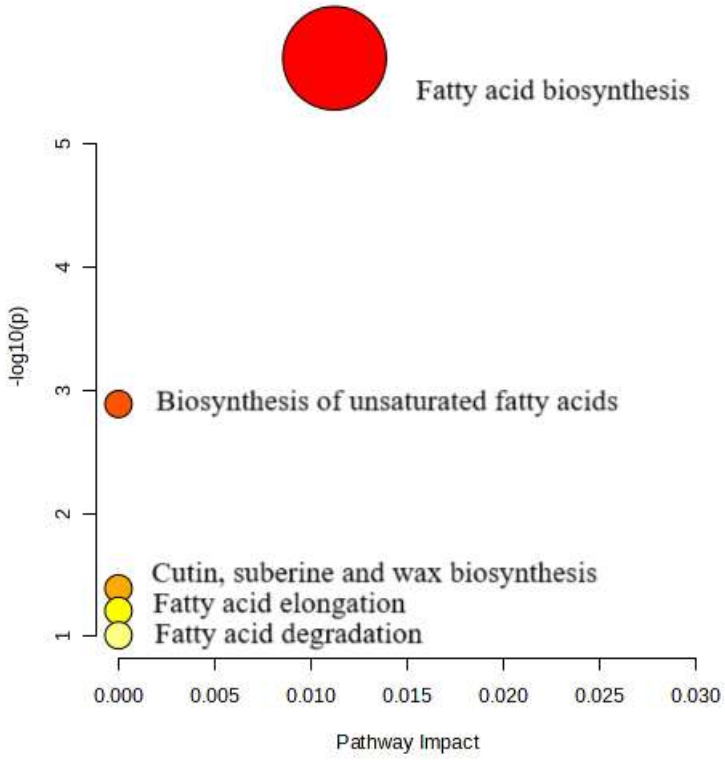

Figure 5. The main metabolite pathway.

2.5. AOAs of Es, Cs, RCs, and four CMs

In the DPPH and ABTS assays, only the IC50 of vitamin C (Vc) was directly detected, while the IC50 of other samples was deduced from the results obtained (Supplemental Table S3).

In the DPPH assay (Figure 6), among the nine samples, RC10 exhibits the highest radical scavenging activity (RSA) at 14.7% in a concentration of 110 μg·mL^{-1}. PA demonstrates some AOAs at a concentration of 100 μmol·L^{-1}, but its RSA values become negative as the concentration increases. The RSA values of OA and LA in the high concentration group show a positive correlation with concentration, although the initial value of OA is negative. At 1200 mmol·L^{-1}, the RSA value of OA is 6.39%, whereas that of LA is 35%. Vc demonstrates the lowest IC50 value, indicating the strongest antioxidant effect.

 doi:10.20944/preprints202402.0584.v1

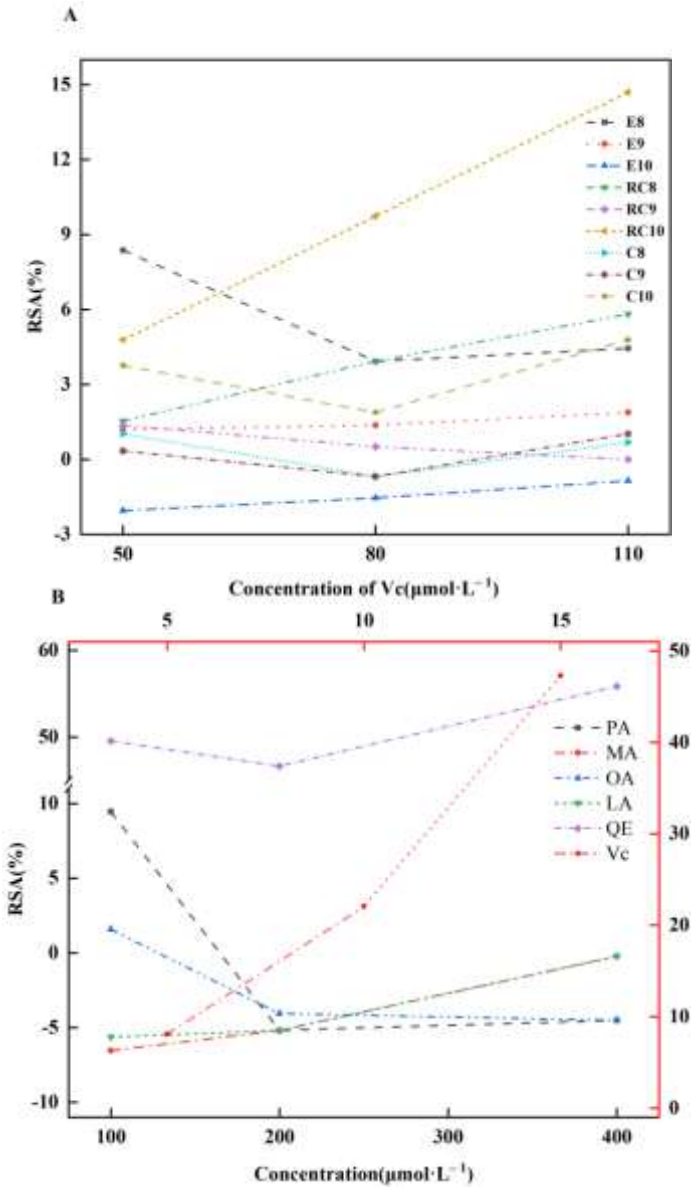

Figure 6. A: RSA of Es and their separated parts. B: RSA of four CMs and two references. QE: quercetin.

The ABTS assay (Figure 7) reveals that the RSA values of RCs are generally higher than those of the corresponding Es or Cs, indicating that the Cs may contain compounds with antagonistic AOA. Interestingly, the IC50 value of Vc is higher in the ABTS assay compared to the DPPH method, while the IC50 value of QE is lower in the ABTS assay. It is important to note that most of the samples exhibit improved RSA values when compared to the results obtained from the DPPH assay. This improvement can be attributed to the higher reactivity of ABTS radical cations [27].

Preprints.org (www.preprints.org) | NOT PEER-REVIEWED | Posted: 9 February 2024 doi:10.20944/preprints202402.0584.v1

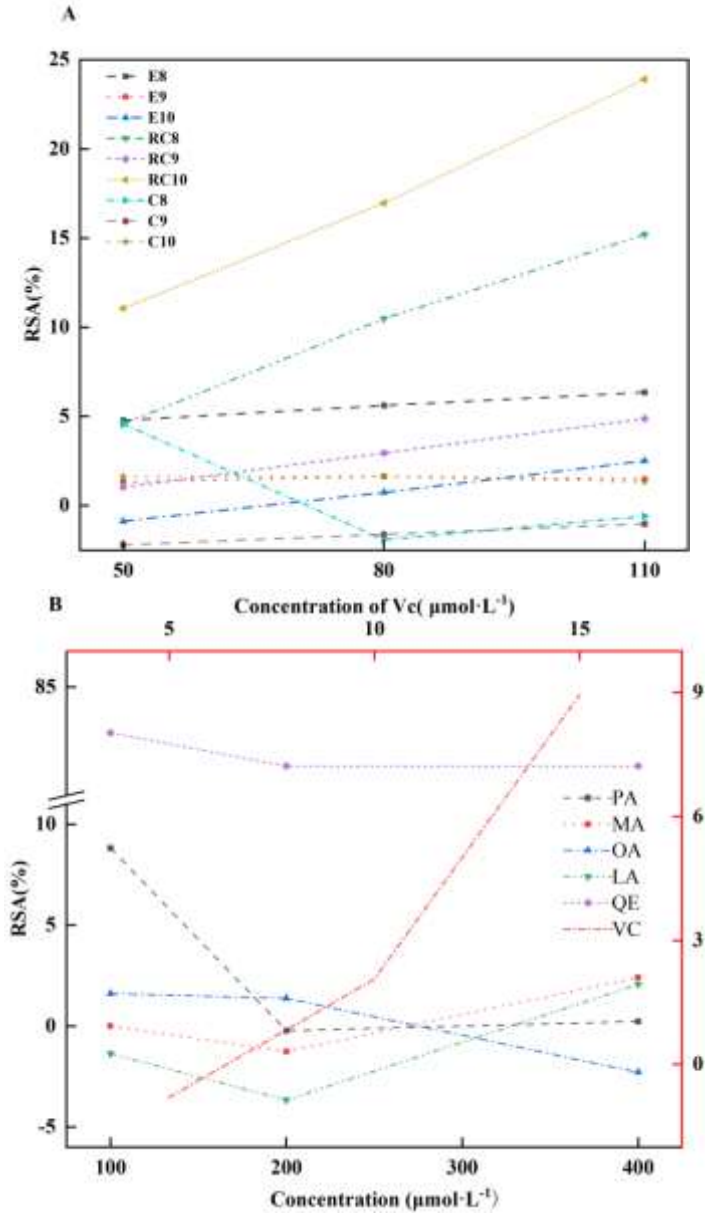

Figure 7. A: RSA of Es and their separated parts. B: RSA of four CMs and two references.

In the FRAP assay, the AOAs are measured based on the concentration of Fe^{2+} (mmol·L^{-1}). At a concentration of 300 mmol·L^{-1}, the FRAP values of OA and LA are significantly higher than that of Vc at 15 μmol·L^{-1}, and similar to that of QE at 200 and 100 μmol·L^{-1}, respectively. However, as the concentration increases to 600 and 1200 mmol·L^{-1}, the FRAP values of OA and LA gradually decrease. It is noteworthy that the FRAP values of nine samples are similar to that of Vc at 10 μmol·L^{-1}.

Overall, OA and LA exhibit some pro-oxidation activities (POAs) in the lower concentration group, but demonstrate good AOAs in the higher concentration group.

3. Discussion

3.1. Extraction and separation

The average yield of 0.11% is in close agreement with the previously reported yield of 0.1% [9]. However, these yields are relatively lower compared to those of *Citrus* and Lamiaceae (*Lavandula dentata*, *Mentha spicata*, *Origanum vulgare*, *Rosmarinus officinalis*, and *Thymus vulgaris*) [11–13]. This can

 doi:10.20944/preprints202402.0584.v1

be attributed to the abundance of compounds with high boiling points (BP) in the Es of PR, such as LCFAs and their esters.

3.2. Chemical composition of the Es from PR

The excess dilution of the samples has led to the detection of only several peaks in the TIC obtained by GC-MS using a DB-5 column. This, in turn, affects the accuracy of chemical identification and quantitation to some extent.

The Es are primarily composed of LCFAs, which is consistent with previous reports [9,10]. The Cs and RCs also consist mainly of LCFAs. The Cs contain a relatively higher content of PA, while the RCs have a relatively lower content of PA compared to the Es. In terms of the AMs, previous reports have only mentioned the presence of linalool in the leaf of PR [10]. The Es from *C. reticulata* (usually more than 1%), *O. vulgare* (11.23%), and *T. vulgaris* (12.02%) also exhibit relatively high contents of linalool [11–13]. It is worth noting that 1-octene-3-ol is known for its distinctive mushroom flavor [30].

The mass spectra of compounds F14, F15, and F16 closely resemble those of LA, OA, and stearic acid, respectively. However, their LRIs^{d} values of 2884, 2770, and 2700 are significantly different from the corresponding LRIs^{c} values recorded in the NIST17 database, which are 3164, 3173, and 3136, respectively. Considering the MS oven temperature program of FFAP, the maximum calculated LRIs^{d} value is 2984. This suggests that chemicals with LRIs^{c} values higher than 2984, such as LA, OA, and stearic acid, will not be eluted under the employed analytical conditions and will be eluted in the subsequent chromatogram, which can significantly alter their LRIs^{d} values. The absence of these compounds in the first detected sample, such as E8, supports this hypothesis. Consequently, the compounds F14, F15, and F16 are still identified as LA, OA, and stearic acid, respectively, consistent with previous reports [9,10].

Although the contents of limonene and α-terpineol are relatively high in the total ion chromatograms (TICs) detected by GC-MS using DB-5, it is worth noting that previous studies [9,10] did not detect these compounds. It is possible that these compounds were introduced from the EOs extracted from the peels of Nanfengmiju (*C. kinokuni*), which were studied simultaneously [11]. Furthermore, it is likely that the compounds such as β-pinene, β-myrcene, *p*-cymene, γ-terpinene, isoterpinolene, and terpinen-4-ol were also introduced from the these EOs. These compounds are commonly found in *Citrus* EOs [11].Based on the percentages, seven compounds, namely PA, MA, LA, OA, methyl palmitate, hexahydrofarnesyl acetone, and phytol, can be chosen as the CMs in these Es.Although their content is relatively low, the C13-norisoprenoids play a significant role in the flavor of Es [31]. Among these compounds, *trans*-β-damascenone is recognized as one of the most important natural aroma compounds and is widely used in the international perfume industry [32]. It possesses a distinctively sweet, fruity, and warm flavor [33]. Additionally, *trans*-β-damascenone has very low odor thresholds, with values of 0.002 $\mu g \cdot L^{-1}$ in water and 5 $\mu g \cdot L^{-1}$ in 25% alcohol [31,33]. This means that only trace amounts are needed to produce an odor [34]. Therefore, *trans*-β-damascenone is likely to make a significant contribution to the unique aroma of Es extracted from PR in this study.

trans-β-Damascenone is primarily formed through the degradation of precursors when heated under acidic conditions [31,35]. In this study, it is likely that *trans*-β-Damascenone was produced from the progenitors during the process of hydro-distillation [36]. Similar mechanisms have been observed for the generation of other volatile C13-norisoprenoids [31,36]. The compound 5β, 6α-dihydroxy-3β-(β-D-glucopyranosyloxy)-7-megastigmen-9-one, which is the only C13-norisoprenoid previously isolated from PR [8], can act as a potential precursor for the synthesis of the seven types of C13-norisoprenoids discovered in this study (Figure 8).

Preprints.org (www.preprints.org) | NOT PEER-REVIEWED | Posted: 9 February 2024 doi:10.20944/preprints202402.0584.v1

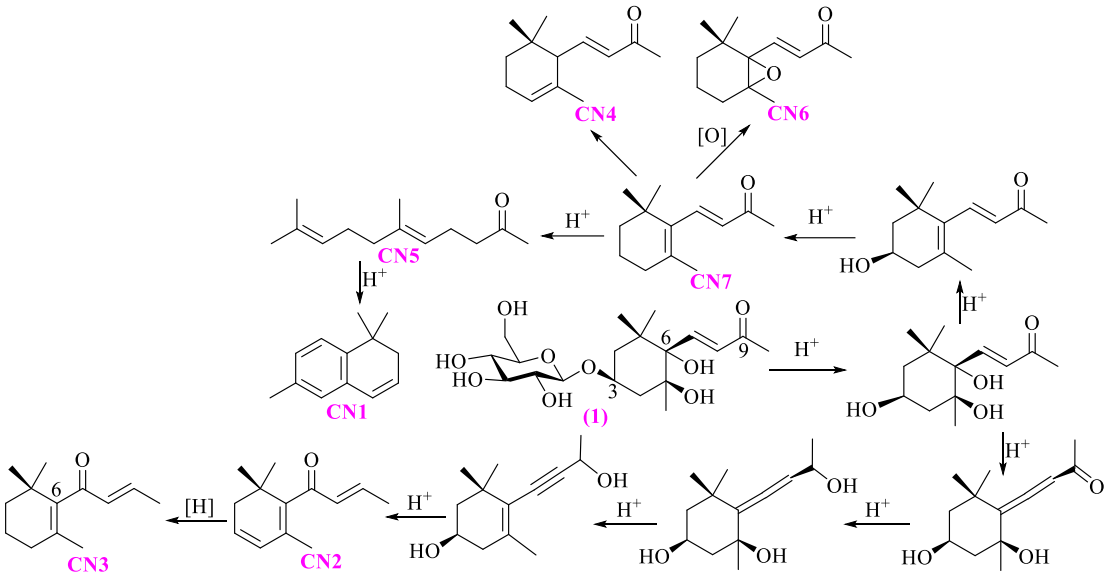

Figure 8. The hypothetical transformation process from 5*β*, 6*α*-dihydroxy-3*β*-(*β*-D-glucopyranosyloxy)-7-megastigmen-9-one **(1)** to seven different types of C13-norisoprenoids.

The Es extracted from PR exhibit certain similarities to the Es extracted from *M. sylvestris* [37], *Cirsium japonicum* var. *ussurience* Kitamura, *Ixeris dentate*, and *I. stolonifera* [38,39]. This similarity is attributed to the presence of high BP compounds such as PA and hexahydrofarnesyl acetone, which are major components in all these extracts.

3.3. PCA and PLS-DA results

After considering the screened 50 compounds based on their VIP values, the compounds represented in the loadings of the PCA plot, the eight compounds identified by GC-MS using DB-5 column, and the content of the compounds, the following nine chemicals have been identified as the CMs: PA, *trans*-*β*-Damascenone, Hexahydrofarnesyl acetone, MA, Phytol, Hexanal, LA, OA, and Methyl palmitate.*3.4. Metabolic pathway analysis*

In Figure 9, the biosynthesis of each CM has been depicted based on the deduced metabolite pathway, which includes fatty acid biosynthesis, biosynthesis of unsaturated fatty acids, fatty acid elongation, fatty acid degradation, and linoleic acid metabolism, listed in sequential order.

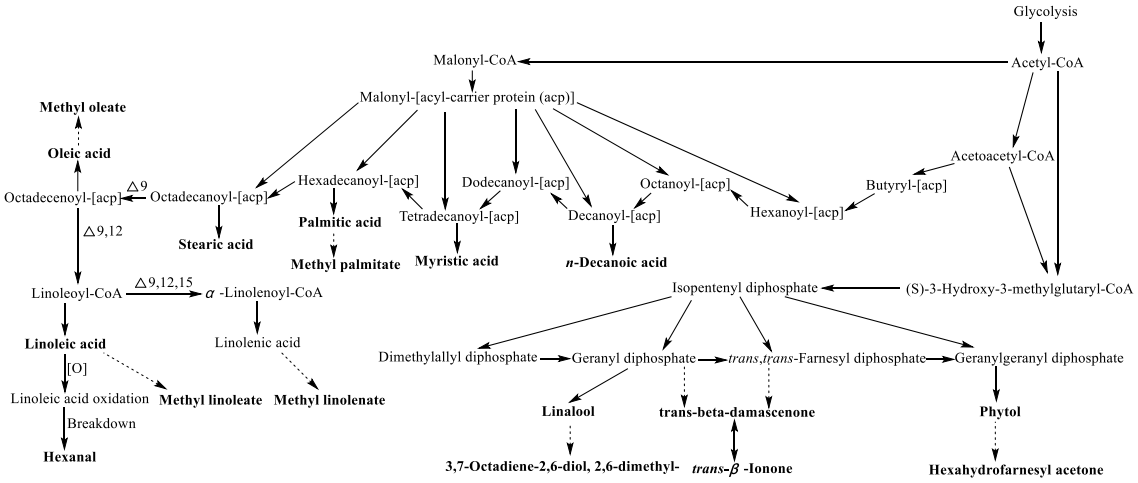

Figure 9. The biosynthesis of CMs. The dashed line arrow indicates that the transformation has been inferred by the authors.

 doi:10.20944/preprints202402.0584.v1

3.5. AOAs of Es, Cs, RCs, and four CMs

There are several methods available to assay the AOAs of chemicals, including DPPH, ABTS, and FRAP. While these methods share a similar principle, they have their own advantages and disadvantages [40]. Therefore, it is recommended to utilize at least two different methods to assess the AOAs of chemicals. It is important to note that even slight variations in experimental procedures can lead to significant differences in the obtained results. The outcomes of these assays are highly influenced by various factors [40]. Therefore, it is challenging to achieve identical results under strictly "equal conditions".

In the DPPH and ABTS methods, the RCs generally exhibit higher AOAs compared to the corresponding Es and Cs. This difference in activity is likely attributed to the higher content of PA in the Cs. In some cases, the Cs may even display POAs. It is worth noting that PA, as a member of SFAs, can induce oxidative stress, inflammation, insulin resistance, and impair endothelial function in a concentration-dependent manner [19–24,41,42].

For instance, at higher concentrations (400 μM), PA not only increases oxidative stress injury but also induces overexpression of the $P66^{Shc}$ protein. However, at lower concentrations (200 μM), PA only slightly increases the expression of $P66^{Shc}$ protein [23]. $P66^{Shc}$ protein plays a role in promoting oxidation and apoptosis by regulating ROS production [42]. In this study, the RSA values of PA also demonstrate a concentration-dependent trend.

Regarding the AOAs of MA, previous studies have provided conflicting results. On one hand, MA can significantly stimulate human polymorphonuclear leukocytes, which play a crucial role in defending against microbial infections, to produce ROS. Excessive intake of MA can lead to detrimental consequences due to uncontrolled ROS production [43]. On the other hand, MA has been shown to protect the testes against oxidative stress caused by hyperglycemia [44]. In this study, MA exhibits weak AOAs or some POAs at concentrations of 100, 200, and 400 $\mu mol \cdot L^{-1}$. Further research is needed to determine the circumstances under which MA exhibits AOAs or POAs.

OA has been shown to prevent the production of ROS in the endoplasmic reticulum and to inhibit endoplasmic reticulum stress-induced inflammatory responses while also altering membrane lipid peroxidation [45,46]. Both OA and LA are capable of exerting AOAs by reducing pro-inflammatory signals [47]. Interestingly, in this study, LA exhibits better AOAs compared to OA in the higher concentration group, which may be attributed to the number and conjugation of double bonds present in LA and OA [48,49]. Generally, PUFAs with more double bonds and conjugations tend to exhibit better AOAs [19–22,48,49], as the ROS have a tendency to react with the loosely bound electrons of the carbon double bonds, which are abundant in the fatty acyl chains of cell membrane lipid bilayers [17]. However, it is important to note that an increased number of double bonds and conjugations also means that PUFAs are more susceptible to reaction with oxygen and the generation of ROS [50,51]. Therefore, LA can be utilized as a free radical product to evaluate the AOAs of compounds [50]. Furthermore, it has been observed that linolenic acid (l8:3, n-6) and eicosatrienoic acid (20:3, n-3) can enhance oxidant injury [18]. Excessive intake of MUFAs and PUFAs can also lead to oxidative stress and inflammation in *in vivo* models [52]. The relationship between the degree of unsaturation and susceptibility to oxidant injury remains unclear [17].

The *in vitro* study showed that SFAs caused significant cellular lipotoxic damage, while the combination of MUFAs/PUFAs with SFAs greatly improved the impaired cell viability [53]. However, in this study, we did not detect any synergistic AOAs of the four CMs. Additionally, the RSA values of RC10 are significantly higher than those of the other eight samples. This suggests that RC10 possesses unique biological activities that warrant further investigation.

 doi:10.20944/preprints202402.0584.v1

4. Materials and Methods

4.1. Plant Materials, Reagents and Chemicals

The aboveground portion of PR was collected from three populations: L8, L9, and L10. These populations corresponded to the same sample numbers used in a previous research study [25]. The authenticity of the collected populations was confirmed by Professor Yi Zhang, from the Chengdu University of Traditional Chinese Medicine (CUTCM), Chengdu, China, and using internal transcribed spacer 2 (ITS2) DNA barcodes, as described in the previous study [25]. Voucher samples of L8, L9, and L10 were deposited in the College of Ethnic Medicine at CUTCM, Chengdu, China, and the Chongqing Academy of Chinese Materia Medica, Chongqing, China.

Table 1. The origins of PR and the corresponding GenBank accession numbers of the ITS2 sequences, as mentioned in the previous study [25].

Voucher No.	Sources	GPS Coordinates	GenBank Accession Number
L8 L9 L10	BianBa, LeiWuQi and NaQu counties of Tibet	E: 93° W: 31°	KP699743/45-4750-51/54

The following reagents and chemicals were used in this study: *n*-hexane (high-performance liquid chromatography grade), linalool (98%+), *p*-cymene (99%+), *α*-terpineol, and nonane (98%) (98%+), which were produced by Adamas Reagent Company Ltd.; *d*-limonene (96%) produced by Acros Organics, USA; *γ*-terpinene (97%) produced by Wako Pure Chemical Industries, Ltd., Japan; PA produced by CATO; *n*-alkanes standard solution of C10-C25 produced by Dr. Ehrenstorfer Inc, Germany; *n*-octacosane (99%) produced by Aldrich; DPPH, ABTS powder, potassium persulfate ($K_2S_2O_8$), and Vc. All these reagents and chemicals were supplied by Shanghai Titan Scientific Co.,Ltd., China.

4.2. Extraction and separation

Weighed powders of L8, L9, and L10 (315 g each) were placed in separate round-bottomed flasks. Pure water (3150 mL, 10 volumes) was added to each flask. The mixtures were soaked for 0.5 hours at 40 °C. The Es were extracted three times from each powder using hydrodistillation with a Clevenger-type apparatus. Each extraction lasted for 5 hours. *n*-Hexane was employed as the collecting solvent. The collected Es, which appeared as light yellow, were treated with anhydrous Na_2SO_4 to eliminate any residual water.

To evaluate crystallization, the Es of L8, L9, and L10 were stored at different temperatures: 4 °C, -4 °C, and -80 °C. Cs were obtained either at 4 °C or -4 °C. However, at -80 °C, the RCs of all three samples were in a solid state. Therefore, there were three sets of samples for L8, L9, and L10: E, C, and RC. Specifically, there were nine samples: E8, E9, and E10, C8, C9, and C10, RC8, RC9, and RC10. Each sample was stored in separate screw-capped vials at 4 °C.

4.3. The identification and quantitation of chemicals in the Es, Cs, and RCs

4.3.1. Sample preparation

The samples of E8, E9, E10, C8, C9, C10, RC8, RC9, and RC10 were prepared for analysis as follows: For GC-FID and GC-MS detection using a DB-5 column (30 m×0.25 mm i.d., 0.25 μm film thickness), the samples were diluted in the ratio of V_{sample}: $V_{n\text{-hexane (HPLC)}}$ 1:1000 (0.1%). For GC-MS detection using a FFAP column (30 m×0.32 mm×0.5 μm), the samples were diluted in the ratio V_{sample}: $V_{n\text{-hexane (HPLC)}}$ 1:250 (0.4%).

 doi:10.20944/preprints202402.0584.v1

4.3.2. GC analyses

GC analyses were performed using the prepared samples. During the analyses, the retention times and peak areas of the compounds were recorded. The obtained chromatograms and mass spectra were analyzed to identify and quantify the target compounds present in the samples.

GC-FID analyses were conducted using a GC-2010 instrument from Shimadzu, Japan, equipped with a DB-5 column. The following parameters were used: The oven temperature was programmed from 60 °C with a 3-minute hold, and then ramped up to 250 °C at a rate of 2.5 °C per minute. The final temperature was held for 2 minutes. Nitrogen was used as the carrier gas, with a constant flow rate of 1.7 mL per minute. Both the injector and the detector were maintained at 250 °C. The sample was split in a ratio of 5:1. Each sample was injected once with a volume of 1 µL.

GC-MS analyses were performed using a GCMS-TQ8040 instrument from Shimadzu, Japan. Separately, either a DB-5 column or a FFAP column was used for the GC-MS analyses. The following parameters were used.

For DB-5 column analysis: The oven temperature was programmed from 60 °C with a 3-minute hold, and then ramped up to 280 °C at a rate of 2.5 °C per minute. The final temperature was held for 2 minutes. Helium was used as the carrier gas, with a constant flow rate of 1 mL per minute. The sample was split in a ratio of 100:1. A solvent delay of 3.0 minutes was implemented. The injector was maintained at 250 °C, while the ion-source and interface were maintained at 200 °C and 250 °C, respectively. Mass spectra were acquired at 70 eV with a scan rate of 3.9 scans per second, covering the mass range from m/z 25 to 450 amu. Each sample was injected once with a volume of 1 µL.

For FFAP column analysis: The oven temperature was programmed from 60 °C with a 3-minute hold, and then ramped up to 230 °C at a rate of 2.5 °C per minute. The final temperature was held for 2 minutes. The rest of the parameters (carrier gas, splitting ratio, solvent delay, injector, ion-source, interface temperature, mass spectra, injection times, and injection volume) remained the same as for the DB-5 column analysis.

4.3.3. Identification and Quantitation

4.3.3.1. Identification

For compound identification, either a NIST 14 or a NIST 17 MS database was utilized. Initially, the peaks in the TICs were identified using probability-based matching. However, due to the presence of overlapped and embedded peaks in the TICs, the identification results may sometimes be inaccurate. In such cases, characteristic ion peaks were selected and compared with the NIST 14 or 17 database, as well as the mass spectra of known standards. By employing a combination of probability-based matching and comparing characteristic ion peaks, the compound identification process becomes more reliable, particularly when dealing with complex samples with overlapping peaks. This approach enhances the overall accuracy and confidence in the identification results.

The LRI value was calculated using the equation (1) proposed by Van Den Dool and Kratz [54]. In equation (1), "t_n" and "t_{n+1}" represent the retention time (RT) of the *n*-alkanes (C10-C25, C28, and the detected C26-C27, C29) with the corresponding number ("n") of carbons. "t_x" represents the RT of the detected compound x (t_x), where "$t_n \leq t_x \leq t_{n+1}$". Furthermore, the RT of *n*-alkane C30 (t_{30}) was deduced by analyzing the TIC obtained through GC-MS using the FFAP column.

$$LRI=100n+100[(t_x-t_n)/(t_{n+1}-t_n)] \quad (1)$$

The calculated LRIs^{b1}, LRIs^{b2}, and LRIs^{d}, which correspond to the RTs detected in GC-FID using a DB-5 column, GC-MS using a DB-5 column, and GC-MS using a FFAP column, respectively, were compared with the LRI^{a} and LRI^{c} recorded in the NIST 17 MS database for the corresponding identified chemicals.

4.3.3.2. Quantification

The relative area percentage of each compound was calculated using peak area normalization.

 doi:10.20944/preprints202402.0584.v1

4.4. PCA and PLS-DA

In R version 4.3.1, the plots of VIP, PCA, PLS-DA for the nine samples and chemicals were generated. Variables with a VIP score greater than 1 are considered significant. The selection of compounds was based on the criteria that the VIP score > 1 and a significance level of $P \leq 0.05$.

4.5. Metabolic pathway analysis

The metabolic pathway analysis of the CMs was performed using MetaboAnalyst 6.0, a web-based tool (https://www.metaboanalyst.ca/), as well as the KEGG system (https://www.kegg.jp/kegg/). Specifically, the results of the metabolic pathway analysis were visualized in "Figure 5", which was generated using MetaboAnalyst 6.0.

4.6. AOAs of Es, Cs, RCs, and four CMs

The AOAs of nine samples, E8, E9, E10, C8, C9, C10, CF8, CF9, and CF10, were tested by DPPH, ABTS, and FRAP assays, respectively.. In addition, four CMs including PA, MA, OA, and LA, as well as two reference compounds, Vc and QE, were also included in the analysis.

4.6.1. Sample preparation

All the subjects were diluted in methanol (MeOH). Since there was a limited amount of volatile oils available, only three low concentrations, namely 50, 80, and 110 $\mu g \cdot mL^{-1}$, were set up for the nine samples of Es, Cs, and RCs. The four CMs (PA, MA, OA, LA) and the reference compound QE were diluted to specific concentrations of 100, 200, and 400 $\mu mol \cdot L^{-1}$, respectively. In the case of OA and LA, an additional higher concentration group was established, with concentrations of 300, 600, and 1200 $mmol \cdot L^{-1}$. Furthermore, the reference compound Vc was diluted to concentrations of 5, 10, and 15 $\mu mol \cdot L^{-1}$ for the analysis.

4.6.2. DPPH assay

A slight modification was made to the experimental procedure[55]. A volume of 100 µL of the sample at various concentrations was added to individual wells of a 96-well microplate. Subsequently, 100 µL of DPPH solution (100 $\mu mol \cdot L^{-1}$) also diluted with MeOH was added to each well. The microplate was then incubated in darkness at room temperature for 30 minutes. After the incubation period, the absorbance of the reaction mixture was measured at 517 nm using a microplate reader. Each sample was analyzed in triplicate, and MeOH was used as the blank control. The RSA was calculated using the following equation:

$$RSA\ (\%)=[(A_{Blank}-A_{Sample})/A_{Blank}]*100\% \quad (2)$$

Where A_{Blank} is the absorbance of the blank control (MeOH) and A_{Sample} is the absorbance of the reaction mixture. The RSA value indicates the percentage of DPPH radical scavenged by the sample, with higher values indicating stronger antioxidant activity.

4.6.3. ABTS assay

A slight modification was made to the method described in a previous study [56]. To prepare the ABTS radical cation ($ABTS^{\bullet+}$) solution, 5 mL of a 7 mM aqueous ABTS solution was reacted with 88 µL of a 140 mM $K_2S_2O_8$ aqueous solution (resulting in a final concentration of 2.45 mM for $K_2S_2O_8$). The reaction mixture was kept in darkness at room temperature for 16 hours. Subsequently, the radical cation solution was diluted with MeOH, typically around 30-50 times, until its absorbance reached a value of 0.7±0.02 at 734 nm. For each sample, 100 µL was added to 100 µL of the ABTS radical solution. The mixture was thoroughly mixed at room temperature for 6 minutes. Following the incubation period, the absorbance at 734 nm was measured using a microplate reader. The calculation method for RSA was consistent with that used in the DPPH assay.

 doi:10.20944/preprints202402.0584.v1

4.6.4. FRAP assay

A slight modification was made to the method described previously [53]. For each sample, 100 μL was added to 100 μL of the FRAP working solution. The FRAP working solution was composed of acetic acid buffer (0.3 mol·L^{-1}), TPTZ (2, 4, 6-Tris (2-pyridyl)-1, 3, 5-triazine) solution (10 mM), and $FeCl_3$ (20 mM) solution, with a volume ratio of 10:1:1. The sample and the FRAP working solution were thoroughly mixed and then placed in darkness at 37 °C for a 30-minute incubation period. After incubation, the absorbance of the mixture at 593 nm was immediately measured using a microplate reader. The increase in absorbance at this wavelength indicates the reduction capacity of the samples and provides information on their antioxidant potential.

To establish a calibration curve, 0.1 mL of Fe(II) aqueous solutions with concentrations ranging from 0.01 to 0.2 mM were mixed with 0.1 mL of the FRAP reagent. In this measuring system, the total antioxidant capacity was determined in terms of Fe(II) equivalents. The concentration of $FeSO_4$ (in mmol·L^{-1}) was calculated based on the absorbance value obtained from the standard curve after the reaction, which was referred to as the FRAP value. A higher FRAP value indicates a stronger antioxidant activity.

5. Conclusions

A comprehensive analysis of the Es of PR has revealed a total of 107 identified and quantified compounds. Among these compounds, 76 have been reported for the first time from the Es of PR. Based on their content, seven compounds, including PA, MA, LA, OA, methyl palmitate, hexahydrofarnesyl acetone, and phytol, have been selected as CMs. Additionally, *trans-β*-damascenone has been chosen as a CM based on its distinct flavor profile. In summary, these eight compounds and hexanal have been identified as the CMs in the Es of PR. Metabolic pathways related to these CMs include fatty acid biosynthesis, biosynthesis of unsaturated fatty acids, cutin, suberine and wax biosynthesis, fatty acid elongation, and biosynthesis of terpenoids. The interplay and relationships between these metabolic pathways have also been depicted.

Interestingly, RCs have demonstrated stronger AOAs, while Cs have shown weaker AOAs compared to Es in general. This disparity is likely influenced by the varying content of PA in these samples. Specifically, the percentage of PA, the most abundant compound, has been found to be higher in Cs but lower in RCs compared to Es.

The accuracy of chemical identification and quantification was somewhat affected due to the inappropriate dilution of samples. Furthermore, no synergistic AOAs were detected in the screened CMs. In future research, we should exercise caution during sample dilution and to place a stronger emphasis on investigating the synergistic effects of CMs, particularly focusing on samples that exhibit stronger AOAs.

This study significantly contributes to our understanding of the composition of the Es of PR, shedding light on the potential applications and utilization of these volatile oils, which are rich in LCFAs.

Supplementary Materials: The following supporting information can be downloaded at the website of this paper posted on Preprints.org.

Author Contributions: Conceptualization, Z.P. and J.W.; methodology, C.X. and J.W.; software, C.X., J.L., X.Y., A.H. and J.W.; validation, Z.P., C.X., X.Y., Y.S., A.H. and J.W.; investigation, C.X. and J.W.; resources, Z.P.; data curation, C.X., X.Y. and J.W.; writing—original draft preparation, C.X., J.L., X.Y. and J.W.; writing—review and editing, Z.P., C.X., X.Y., Y.S., A.H., N.M.K., S.A. and J.W.; supervision, Z.P. and J.W.; project administration, Z.P. and J.W.; funding acquisition, Z.P. and J.W. All authors have read and agreed to the published version of the manuscript.

Funding: This research project received funding from several sources, including the National Natural Science Foundation of China (Grant No. 81973567), the Chongqing Science and Technology Bureau and Chongqing Education Commission (Grant No. CSTB2023NSCQ-LZX0046), the Chongqing Science and Technology Bureau (Grant No. cstc2020jcyj-msxmX0310), and the Chongqing Municipal Health Commission (Grant No. 2020ZY023793 and ZY201602104).

 doi:10.20944/preprints202402.0584.v1

Acknowledgments: The authors thank the undergraduates, Hang Shi, Qin Duan, Meiying Luo, Shanshan Jiang, and Churui Xiao, for their contributions.

Conflicts of Interest: The authors declare no conflict of interest.

References

1. Mathiesen, C.; Scheen, A.C.; Lindqvist, C. Phylogeny and biogeography of the lamioid genus *Phlomis* (Lamiaceae). *Kew Bull.* **2011**, *66*, 83–99.
2. The editorial board of Flora of China of Chinese Academy of Sciences. *Flora of China* (in Chinese, Volume 65 issue 2). Science press; Beijing, China, 1977; p. 1, 480.
3. Li, H.; Hedge, I.C. *Flora of China* (*Lamiaceae*) (Volume 17). Science press; Beijing, China, 1994; p. 50, 52, 156-157.
4. Pharmacopoeia committee of the People's Republic of China. *Pharmacopoeia of the People's Republic of China* (Volume I). China Medical Science and Technology Press; Beijing, China, 2020; p. 274.
5. Nanjing University of Chinese medicine. *The dictionary of Chinese materia medica* (Volume 2) - 2nd edition. Shanghai scientific and technical publishers, China. 2006; p. 2390-2391.
6. Cui, Z.H.; Qin, S.S.; Qin, E.H.; Qin, C.; Gao, L.; Li, Q.C.; Wang, Y.L.; Huang, X.Z.; Zhang, Z.Y.; Li, M.H. Traditional uses, phytochemistry, pharmacology and toxicology of *Lamiophlomis rotata* (Benth.) Kudo: a review. *RSC Adv.* **2020**, *10*, 11463.
7. Li, Y.; Li, F.; Zheng, T.T.; Shi, L.; Zhang, Z.G.; Niu, T.M.; Wang, Q.Y.; Zhao, D.S.; Li, W.; Zhao, P. Lamiophlomis herba: A comprehensive overview of its chemical constituents, pharmacology, clinical applications, and quality control. *Biomed. Pharmacother.* **2021**, *144*, 112299.
8. Zhang, F.; Wu, Z.J.; Sun, L.; Wang, J.; Tao, X.; Chen, W.S. Iridoid glucosides and a C_{13}-norisoprenoid from *Lamiophlomis rotata* and their effects on NF-kB activation. *Bioorg. Med. Chem. Lett.* 2012, 22, 4447-4452.
9. Liu, H.F.; Li, X.; Deng, Y.; Song, X.; Li, H. Study on the chemical constituents of the essential oil from *Lamiophlomis rotata*. *Chin. J. Pharm. Anal.* **2006**, *26*, 1794-1796.
10. Liu, J.; Nan, P.; Wang, L.; Wang, Q.; Tsering, T.; Zhong, Y. Chemical variation in lipophilic composition of *Lamiophlomis rotata* from the Qinghai-Tibetan plateau. *Chem. Nat. Compd.* **2006**, *42*, 525-528.
11. Wang, J. Alkanes and chemical markers identified in the essential oil from pericarp of Nanfengmiju (*Citrus kinokuni* Hort. ex Tanaka). *J. Mex. Chem. Soc.* **2023**, *67*, 82-93.
12. Ul Haq, A.; Wang, J. Identification of varieties and biomarkers analyses on essential oils from peels of *Citrus* L. collected in Pakistan. *Pak. J. Bot.* **2023**, *55*, 1407-1418.
13. Ali, S.; Seema, H.; Khan, Z.; Din, A.; Hadi, F.; Wang, J. The nomenclature of three *Citrus* varieties collected in Pakistan and chemicals in essential oils from their peels. *Pak. J. Bot.* **2024**, 56, .
14. Jia, Z.P.; Li, M.X.; Zhang, R.X.; Wang, J.H.; Wang, M.; Guo, X.N.; Shen, T. Vitro screening of the effective antitumor components of Herba *Lamiophlomis rotata*. *Med. J. Nation. Defend Force Northwest Chin.* **2005**, *26*, 173-175.
15. Zhou, Z.; Li, T.; Du, R.; Liu, C.; Huang, S.; Han, L.; Zhang, P.; Wang, Y.; Jiang, M. *Lamiophlomis rotata* attenuates rheumatoid arthritis by regulating sphingolipid and steroid hormone metabolism. *Mol. Omics* **2023**, *19*, 72-83.
16. Aebisher, D.; Cichonski, J.; Szpyrka, E.; Masjonis, S.; Chrzanowski, G. Essential oils of seven Lamiaceae plants and their antioxidant capacity. *Molecules* **2021**, *26*, 3793.
17. Hart, C.M.; Tolson, J.K.; Block, E.R. Fatty acid supplementation protects pulmonary artery endothelial cells from oxidant injury. *Am. J. Respir. Cell Mol. BioI.* **1990**, *3*, 479-489.
18. Hart, C.M.; Tolson, J.K.; Block, E.R. Supplemental fatty acids alter lipid peroxidation and oxidant injury in endothelial cells. *Am. J. Physiol.* **1991**, *260*, L481-L488.
19. Kehrer, J.P.; Autor A.P. The effect of dietary fatty acids on the composition of adult rat lung lipids: relationship to oxygen toxicity. *Toxicol. Appl. Pharmacol.* **1978**, *44*, 423-430.
20. Kennedy, J.I.; Chandler, D.B.; Fulmer, J.D.; Wert, M.B.; Grizzle, W.E. Dietary fish oil inhibits bleomycin-induced pulmonary fibrosis in the rat. *Exp.Lung Res.* **1989**, *15*, 315-329.
21. Sosenko, I.R.S.; Innis, S.M.; Frank, L. Polyunsaturated fatty acids and protection of newborn rats from oxygen toxicity. *J. Pediatr.* **1988**, *112*, 630-637.
22. Sosenko, I.R.S.; Innis, S.M.; Frank, L. Menhaden fish oil, n-3 polyunsaturated fatty acids, and protection of newborn rats from oxygen toxicity. *Pediatr. Res.* **1989**, *25*, 399-404.
23. Favre, J.; Yıldırım, C.; Leyen, T.A.; Chen, W.J.Y.; Genugten, R.E.; Golen, L.W.; Garcia-Vallejo, J.J.; Musters, R.; Baggen, J.; Fontijn, R.; Pouw Kraan, T.; Serné, E.; Koolwijk, P.; Diamant, M.; Horrevoets, A.J.G. Palmitic acid increases pro-oxidant adaptor protein p66Shc expression and affects vascularization factors in angiogenic mononuclear cells: Action of resveratrol. *Vasc. Pharmacol.* **2015**, *75*, 7-18.
24. Ke, J.; Wei, R.; Liu, Y. Metformin combined with liraglutide has a synergistic protective effect on palmitic acid-induced oxidative damage of endothelial cells. *Chin. J. Diabetes Mellitus* **2014**, *6*, 312-316.

25. Wang, J.; Gao, Y.L.; Chen, Y.L.; Chen, Y.W.; Zhang, Y.; Xiang, L.; Pan, Z. *Lamiophlomis rotata* identifification via ITS2 barcode and quality evaluation by UPLC-QTOF-MS couple with multivariate analyses. *Molecules* **2018**, *23*, 3289.
26. Adams, R.P. Identification of essential oil components by gas chromatography/mass spectrometry, ed. 4.1. Allured publishing; Illinois, America, 2017; p. 1-804.
27. Flavornet by Terry Acree & Heinrich Arn, https://www.flavornet.org/info/3033-23-6.html (accessed on 3th January 2024).
28. Teow, C.C.; Truong, V.D.; Mcfeeters, R.F.; Thompson, R.L.; Pecota, K.V.; Yencho, G.C. Antioxidant activities, phenolic and β-carotene contents of sweet potato genotypes with varying flesh colours. *Food Chem.* **2007**, *103*, 829-838.
29. Bouzid, H.A.; Oubannin, S.; Ibourki, M.; Bijla, L.; Hamdouch, A.; Sakar, E.H.; Harhar, H.; Majourhat, K.; Koubachi, J.; Gharby, S. Comparative evaluation of chemical composition, antioxidant capacity, and some contaminants in six Moroccan medicinal and aromatic plants. *Biocatal. Agric. Biotechnol.* **2023**, *47*, 102569.
30. Zhao, Q.Y.; Yousaf, L.; Xue, Y.; Shen, Q. Changes in flavor of fragrant rice during storage under different conditions. *J. Sci. Food Agric.* **2020**, *100*, 3435-3444.
31. Carlin, S.; Mattivi, F.; Durantini, V.; Dalledonne, S.; Arapitsas, P. Flint glass bottles cause white wine aroma identity degradation. *PNAS* **2022**, *119*, e2121940119.
32. Pickenhagen, W. In *Flavor Chemistry-Thirty Years of Progress*; Teranishi, R., Wick, E.L., Hornstein, I., Eds. Kluwer Academic/Plenum Publishers: New York, U.S.A, 1999: p. 75-87.
33. Kaneshima, T.; Nojima, S.; Mori, S.; Myoda, T.; Nakahara, K.; Matsuo Y. Isolation and identification of progenitors, glycoconjugates of β-damascenone precursors, in sweet potato (*Ipomoea batatas*). *Flavour Fragr. J.* **2023**, *38*, 152-162.
34. Roberts, D.D.; Mordehai, A.P.; Acree, T.E. Detection and partial characterization of eight β-damascenone precursors in apples (*Malus domestica* Borkh. Cv empire). J. Agric. Food Chem. **1994**, *42*, 345-349.
35. Roberts, D.D.; Roberts, A.P.; Acree, T.E. Detection and partial characterization of eight β-Damascenone precursors in Apples (*Malus domestica* Borkh. Cv. Empire). *J. Agric. Food Chem.* **1994**, *42*, 345-349.
36. Suzuki, M.; Matsumoto, S.; Mizoguchi, M.; Hirata, S.; Takagi, K.; Hashimoto, I.; Yamano, Y.; Ito, M.; Fleischmann, P.; Winterhalter, P.; Morita, T.; Watanabe1, N. Identification of (3*S*, 9*R*)- and (3*S*, 9*S*)-Megastigma-6,7-dien-3,5,9-triol 9-*O*-β-D-glucopyranosides as Damascenone progenitors in the flowers of *Rosa damascena* Mill. *Biosci. Biotechnol. Biochem.* **2002**, *66*, 2692-2697.
37. Usami, A.; Kashima, Y.; Marumoto, S.; Miyazawa, M. Characterization of aroma-active compounds in dry flower of *Malva sylvestris* L. by GC-MS-O analysis and OAV calculations. *J. Oleo Sci.* **2013**, *62*, 563-570.
38. Choi, H.S. GC-MS analyses of the essential oils from *Ixeris dentate* (Thunb.) Nakai and *I. stolonifera* A. Gray. *Korean J. Food Nutr.* **2012**, *25*, 274-283.
39. Choi, H.S. Chemical composition of *Cirsium japonicum* var. *ussurience* Kitamura and the quantitative changes of major compounds by the harvesting season. *Korean J. Food Nutr.* **2016**, *29*, 327-334.
40. Munteanu, I.G.; Apetrei, C. Analytical methods used in determining antioxidant activity: A review. *Int. J. Mol. Sci.* **2021**, *22*, 3380.
41. Fratantonio, D.; Speciale, A.; Ferrari, D.; Cristani, M.; Saija, A.; Cimino, F. Palmitate-induced endothelial dysfunction is attenuated by cyanidin-3-*o*-glucoside through modulation of Nrf2/Bach1 and NF-κB pathways. *Toxicol Lett* **2015**, *239*, 152–160.
42. Giorgio, M.; Migliaccio, E.; Orsini, F.; Paolucci, D.; Moroni, M.; Contursi, C.; Pelliccia, G.; Luzi, L.; Minucci, S.; Marcaccio, M.; Pinton, P.; Rizzuto, R.; Bernardi, P.; Paolucci, F.; Pelicci, P.G. Electron transfer between cytochrome c and $p66^{shc}$ generates reactive oxygen species that trigger mitochondrial apoptosis. *Cell* **2005**, *122*, 221–233.
43. Tada, M.; Ichiishi, E.; Saito, R.; Emoto, N.; Niwano, Y.; Kohno, M. Myristic acid, a side chain of phorbol myristate acetate (PMA), can activate human polymorphonuclear leukocytes to produce oxygen radicals more potently than PMA. *J. Clin. Biochem. Nutr.* **2009**, *45*, 309–314.
44. Khalil, A.S.M.; Giribabu, N.; Yelumalai, S.; Shahzad, H.; Kilari, E.K.; Salleh, N. Myristic acid defends against testicular oxidative stress, inflammation, apoptosis: Restoration of spermatogenesis, steroidogenesis in diabetic rats. *Life Sci.* **2021**, *278*, 119605.
45. Sun, Y.; Wang, J.; Guo, X.; Zhu, N.; Niu, L.; Ding, X.; Xie, Z.; Chen, X.; Yang, F. Oleic acid and eicosapentaenoic acid reverse palmitic acid-induced insulin resistance in human Hepg2 cells via the reactive oxygen species/*Jun* pathway. *Genom. Proteom. Bioinf.* **2021**, *19*, 754–771.
46. Abenavoli, L.; Milanović, M.; Milić, N.; Luzza, F.; Giuffrè, A.M. Olive oil antioxidants and non-alcoholic fatty liver disease. *Expert Rev. Gastroenterol. Hepatol.* **2019**, *13*, 739-749.
47. Pauls, S.D.; Rodway, LA.; Winter, T.; Taylor, C.G.; Zahradka, P.; Aukema, H.M. Anti-inflammatory effects of α-linolenic acid in M1-like macrophages are associated with enhanced production of oxylipins from α-linolenic and linoleic acid. *J. Nutr. Biochem.* **2018**, *57*, 121–129.

 doi:10.20944/preprints202402.0584.v1

48. Wu, S.H.; Sun, G.R.; Wang, Y.Y.; Tan, T.T.; Zhang, Y.; Deng, H.M.; Zhang, T.L.; Du, F.G. Chemical composition analysis and antioxidant activity of essential oil from *Magnolia sieboldii* Leaves. *Mol. Plant Breed.* **2023**, *21*, 1–12.
49. Lee, S.H.; Min, D.B. Effects, quenching mechanisms, and kinetics of carotenoids in chlorophyll-sensitized photooxidation of soybean oil. *J. Agri. Food Chem.* **1990**, *38*, 1630–1634.
50. Sila, A.; Sayari, N.; Balti, R.; Martinez-Alvarez, O.; Nedjar-Arroume, N.; Moncef, N.; Bougatef, A. Biochemical and antioxidant properties of peptidic fraction of carotenoproteins generated from shrimp by-products by enzymatic hydrolysis. *Food Chem.* **2014**, *148*, 445–452.
51. Burton, G.W.; Ingold, K.U. β-Carotene: An unusual type of antioxidant. *Science* **1984**, *224*, 569–573.
52. Grujić-Milanović, J.D.; Miloradović, Z.Z.; Mihailović-Stanojević, N.D.; Banjac, V.V.; Vidosavljević, S.; Ivanov, M.S.; Karanović, D.J.; Vajić, U.-J.V.; Jovović, D.M. Excesive consumption of unsaturated fatty acids leads to oxidative and inflammatory instability in wistar rats. *Biomed. Pharmaco.* **2021**, *139*, 111691.
53. Liu, W.; Zhu, M.; Gong, M.; Zheng, W.; Zeng, X.; Zheng, Q.; Li, X.; Fu, F.; Chen, Y.; Cheng, J.; Rao, Z.; Lu, Y.; Chen, Y.; Comparison of the effects of monounsaturated fatty acids and polyunsaturated fatty acids on liver lipid disorders in obese mice. *Nutrients* **2023**, *15*, 3200.
54. Van Den Dool, H.; Kratz, P.D. A generalization of the retention index system including linear temperature programmed gas-liquid partition chromatography. *J. Chromatogr.* **1963**, *11*, 463-471.
55. Zengin, G.; Sarikurkcu, C.; Uyar, P.; Aktumsek, A.; Uysal, S.; Kocak, M.S.; Ceylan, R. *Crepis foetida* L. subsp. *rhoeadifolia* (Bieb.) Celak. as a source of multifunctional agents: Cytotoxic and phytochemical evaluation. *J. Funct. Foods* **2015**, *17*, 698-708.
56. Re, R.; Pellegrini, N.; Proteggente, A.; Pannala, A.; Yang, M.; Rice-Evans, C. Antioxidant activity applying an improved ABTS radical cation decolorization assay. *Free Radical Bio. Med.* **1999**, *26*, 1231-1237.